We are IntechOpen, the world's leading publisher of Open Access books Built by scientists, for scientists

6,900
Open access books available

185,000
International authors and editors

200M
Downloads

154
Countries delivered to

Our authors are among the

TOP 1%
most cited scientists

12.2%
Contributors from top 500 universities

BOOK CITATION INDEX
CLARIVATE ANALYTICS
INDEXED

WEB OF SCIENCE™

Selection of our books indexed in the Book Citation Index
in Web of Science™ Core Collection (BKCI)

Interested in publishing with us?
Contact book.department@intechopen.com

Numbers displayed above are based on latest data collected.
For more information visit www.intechopen.com

Chloroplast and Mitochondria

Noorah Abdulaziz Othman Alkubaisi
and Nagwa Mohammed Amin Aref

Abstract

Photosynthesis is a crucial process for plants on earth that changes light energy to chemical energy. Virus infection can cause dramatic photosynthesis changes: respiration and the translocation of carbohydrates and other substances around the host plant. Chlorosis in virus-infected leaves like Barley Yellow Dwarf Virus (BYDV- PAV).infection can result from damage to chloroplasts resulting from inhibition of photosynthetic activity. Our present study combines TEM and chlorophyll-level content in the presence of Gold nanoparticles (AuNPS) to explore the repair mechanism for the yellowing leaf symptom development caused by infection with BYDV- PAV by illustrating TEM micrographs; showing fragmentized grana, deformation of the myelin like bodies (MLB), many vesicles; osmiophilic lipid granules/plastoglobulus, starch body, and plasmolysis in the chloroplast, distribution of AuNPs & VLPs near and inside the chloroplast. Mitochondria, Double-membrane-bound organelle, Distorted mitochondrion, Amorphous inclusion bodies.

Keywords: Chloroplast, Barley Yellow Dwarf Virus (BYDV-PAV), Gold nanoparticles (AuNPs), Starch granules (S), osmiophilic lipid granules/plastoglobulus (OG), Myelin like bodies (MLB), Plasmolysis, Portentous content, Fragmentized grana. Mitochondria, Double-membrane-bound organelle, Distorted mitochondrion, Amorphous inclusion bodies

1. Introduction

BYDV-PAV causes cytological alterations, physiological and biochemical, including the restriction of photosynthate transportation, phloem degeneration, and creating a nutritionally [1], and the formation of specific cytological inclusions [2]. In the susceptible wheat and after BYDV-GAV infection, drop expressions of chlorophyll biosynthesis and chloroplast was noticed due to related genes and altered expression of the ABA mentioned above. Chloroplast in the healthy cells has normal densities of thylakoid in chloroplast (**Figure 1(A)–(D)**). The lower chlorophyll content, fragmentized chloroplasts, ROS accumulation, and slower growth could be engaged to ET signaling and ROS related genes, consequently resulting in leaf yellowing and plant dwarfing (**Figure 2**).

Studies by several laboratories of TMV-infected tobacco plants suggest that the uptake of viral CP causes chlorosis in these plants by thylakoid. R. Beachy's lab observed that the CP aggregates in the thylakoid membrane. Resulting the intense free radical damage to the organelle refer to pull apart photosystem II (the water-splitting reaction of photosynthesis). In vitro experiments, M. Zaitlin's laboratory
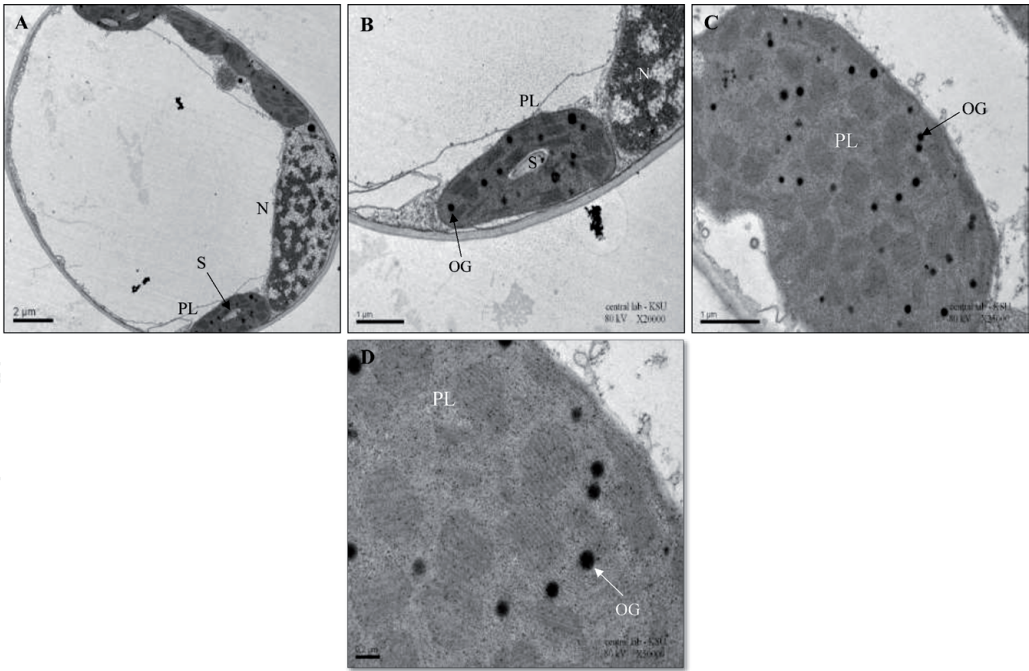
Figure 1.
*Electron micrographs showing a general view inside the healthy cells of barley leaves with densities of thylakoids in chloroplasts. (**A**) The cells show the nucleus and chloroplast with one starch granules, with low magnification, and higher magnification in (**B**), Scale bars 2 µm and 1 µm. (**C**) The outline area shows the inside details of the grana, Scale bar 1 µm. (**D**) The cell shows the plastid contains the osmiophilic lipid granules/plastoglobulus and higher magnification of the grana structure, Scale bar 0.2 µm.*
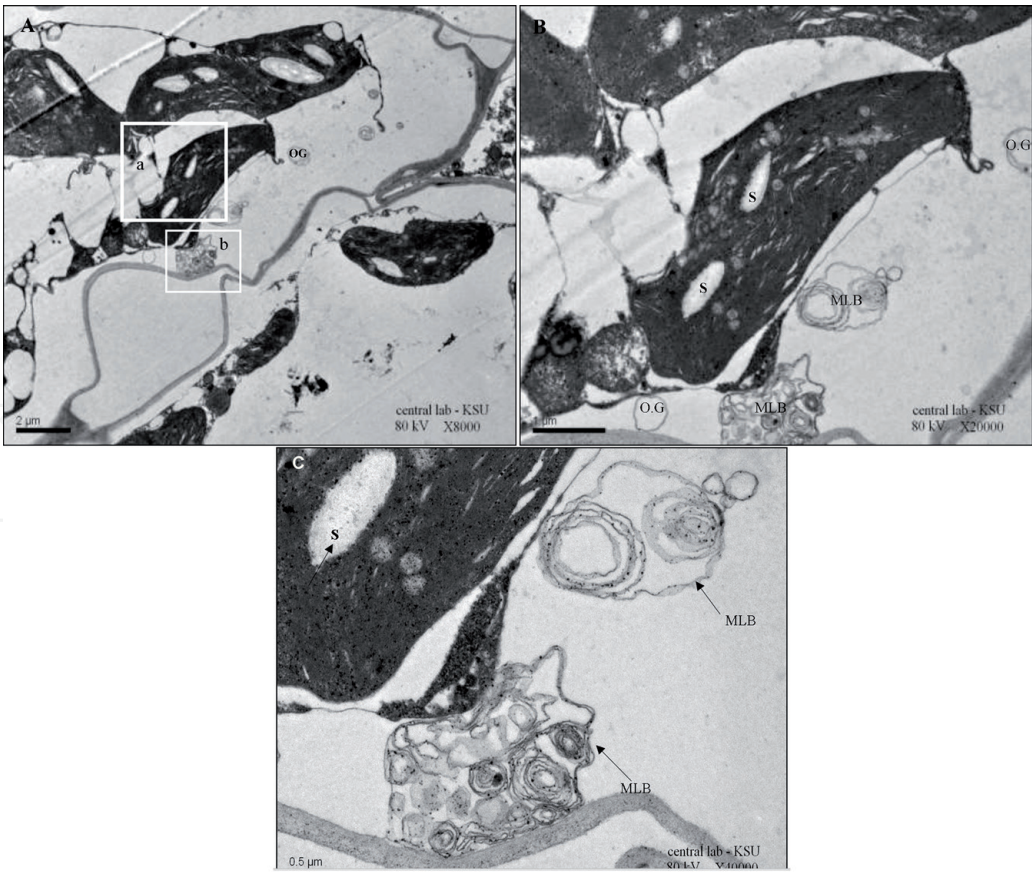

Figure 2.
*Electron micrographs showing fragmentized grana. (**A**) A general view inside the cell infected with BYDV- PAV at lower magnification [outlined area is shown at higher magnification in A]. Scale bar 2 µm. (**B**) Accumulation of starch granules and many osmophilic globules (OGs) is observed in the chloroplast surrounded by bundle sheath cells integrated into the infected cell, Scale bar 1 µm. Electron micrograph showing the deformation of the myelin like bodies (**C**) Numerous intracellular inclusion bodies myelin like bodies (MLB), (arrows), Scale bar 0.5 µm.*

noticed that uptake of the CP did not accomplish the host's normal pathways for protein import using isolated chloroplasts. Instead, a feature of the CP, when it was assembled into multimeric disks (an intermediate structure in TMV virion assembly), let it be taken up randomly into the chloroplasts and the thylakoid membrane eventually. The single amino acid in the CP determines its uptake efficiency into chloroplasts, and K. Lehto has detected the relative severity of chlorosis caused by different TMV strains. Changes in photosynthesis, respiration, and carbohydrate translocation generally cause localized aggregation and depletion of starch, the primary stock carbohydrate of most plants [3]. Common cytopathological effects of BYDV-PAV infection are restricted to the phloem of host plants cleared [4], where they are seen via EM in the cytoplasm, nuclei, and vacuoles of infected sieve elements, companion and parenchyma cells. Vesicles containing filaments and inclusions containing virus particles the infection and subsequent death of phloem cells inhibits translocation as **Figure 2(A)–(C)**, slows plant growth, and induces loss of chlorophyll typical symptoms. Plants convert only 2–4% of the available energy in radiation into new plant growth [5].

2. Chemical energy production of nanoparticles

Metal nanoparticles can induce the efficiency of chemical energy production in photosynthetic systems, **Figure 5(C)**. Nano-anatase TiO2 has a photocatalyzed characteristic, improves the light absorbance, the transformation from light energy to electrical, chemical energy, and induces carbon dioxide assimilation. TiO2NPs protect chloroplast from aging for long time illumination [6, 7]. Nano-anatase TiO2 enhances the photosynthetic carbon assimilation with potentially activate Rubisco (a complex of Rubisco [8], which promotes Rubisco carboxylation, thereby increasing the growth of plants [8, 9] studied the impact of nano-anatase on the molecular mechanism of carbon reaction and postulated the marker gene's induction for Rubisco activase (RCA) mRNA by nano-anatase. Enhancing protein levels and activities of Rubisco activated the improvement of the Rubisco carboxylation and the high rate of photosynthetic carbon reaction. The exogenous application of TiO2NPs improves the net photosynthetic rate, conductance to water, and transpiration rate in plants [10]. Nano-anatase promoted heartily whole chain electron transport [11], photoreduction activity of photosystem II, O2-evolving, and photophosphorylation activity of chlorophyll under both visible and ultraviolet light. The AuNPs and Ag nanocrystals bind to the chlorophyll in the photosynthetic reaction center [12], forming a novel hybrid system, which may build ten times more excited electrons plasmon resonance fast electron–hole separation. The enhancement mechanisms may help the design of artificial light-harvesting systems. Nanomaterials can generate ROS, affect lipid peroxidation, as reported [13]. The significant biochemical and molecular effect on membrane permeability and fluidity, which due to previous nanomaterials impact making cells more susceptible to osmotic stress and failure to nutrient uptake. A series of metabolic activities such as soil and water which perceived the stress through the growth matrix [14–16] triggered to alleviate the metal stressors [17]. To deal with the situation, in the first step, to prohibit metal entry through the expense of energy, plants modulating their action actively. In the second step, modulating transporters in the plasma membrane prevent further entry of the metal into the cytosol, so that the intracellular build-up of metal ions does not exceed the threshold concentration, **Figure 3(A, B,** and **D)**. The plant system has developed several well-synchronized systems to Elementary Flux Mode (EFM) to prevent metal ion build-up from the cellular milieu [18].
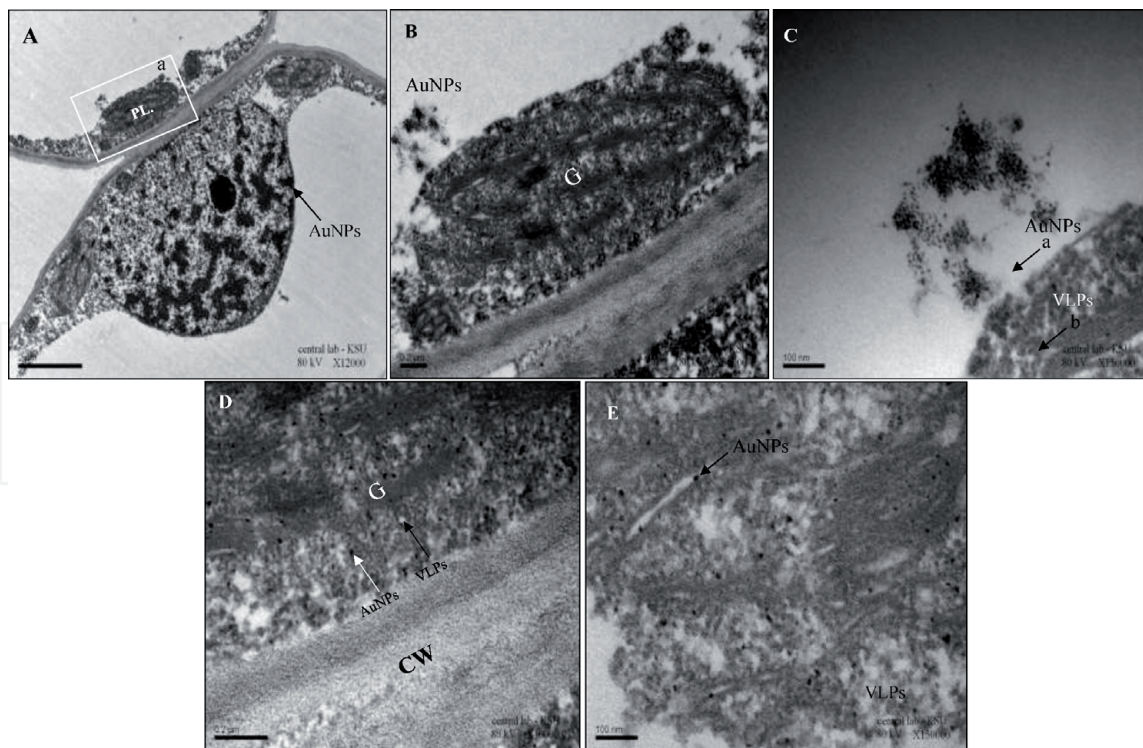
Figure 3.
*Micrographs of a different distribution of AuNPs & VLPs near the chloroplast. (**A**) Micrograph of large nucleus and nucleolus with segregated distinct chromatin beside the cell wall, AuNPs restricted to the chloroplast from both sides, Scale bars 2μm. (**B**) The random bulk number of localized AuNPs aggregated intimately near to the chloroplast; Scale bars 0.2 μm. (**C**) Packed AuNPs in the cytoplasm adjacent to VLPs, Scale bars 100 nm. Micrographs of a different distribution of AuNPs & VLPs inside the chloroplast. (**D**) Dispersed AuNPs into the grana, which appeared to be tiered apart in an unregulated shape, VLPs and AuNPs condensate near the cell wall inside the plastid. Scale bar 0.2 μm. (**E**) Micrographs of the precipitated AuNPs and VLPs between the grana structure. Scale bar 100 nm.*

AuNPs significantly increased vegetative growth and seed production in both noncrops (*Arabidopsis thaliana*) [19] and crop (*Brassica juncea*) species [20]. TEM images revealed that chloroplasts in BYDV-GAV-infected Zhong8601 leaf cells were fragmentized [21] as shown in **Figures 3(A)** and **4(B)** and **(D)** as Where thylakoids were not well developed, but starch granules as in **Figures 3(B, E,** and **F)** and **4(C)** and plastoglobules were not rare in our study. Compared to another strain study for BYDV-GAV [21], mock-inoculated Zhong8601, chlorophyll content was reduced, but the virus and H2O2 contents were markedly higher in BYDV-GAV-infected Zhong860. Reactive oxygen species (ROS)-related genes were transcriptionally regulated in BYDV-GAV infected Zhong8601. These results suggest that the yellow dwarf symptom formation is mainly attributed to reduced chlorophyll content and fragmentized chloroplasts [22]. Phloem damage caused by BYDV limits the transport of photosynthate and restricts long-distance carbohydrate translocation [21]. Carbohydrate accumulation in leaves consecutively inhibits photosynthesis, reduces chlorophyll, and increases respiration [23].

The changes in root system function such as root length or biomass caused by BYDV infection is unknown, although root tips are far from the photosynthate source but suffered from reduced translocation. Potential reductions in root system function of BYDV-infected plants could play a crucial role in grain yield loss because root systems supply shoot organs with fundamental mineral nutrients [24] due to BYDV infection, and a susceptible wheat cultivar showed a 72% reduction in photosynthetic capacity. On the other hand, a moderately tolerant wheat cultivar exhibited only a 60% reduction in photosynthesis [25]. Photosynthesis was reduced by 25% per gram of fresh tissue weight in BYDV-infected plants [26]. Many studies have shown that

virus infection can trigger severe chlorophyll breakdown within the host. An imbalance between biosynthesis and catabolic turnover of green pigments in plant tissues indicates profound inhibition of the photosynthesis process [27–30]. Phytohormone levels are also altered following BYDV infection. [31] undertook a detailed study of
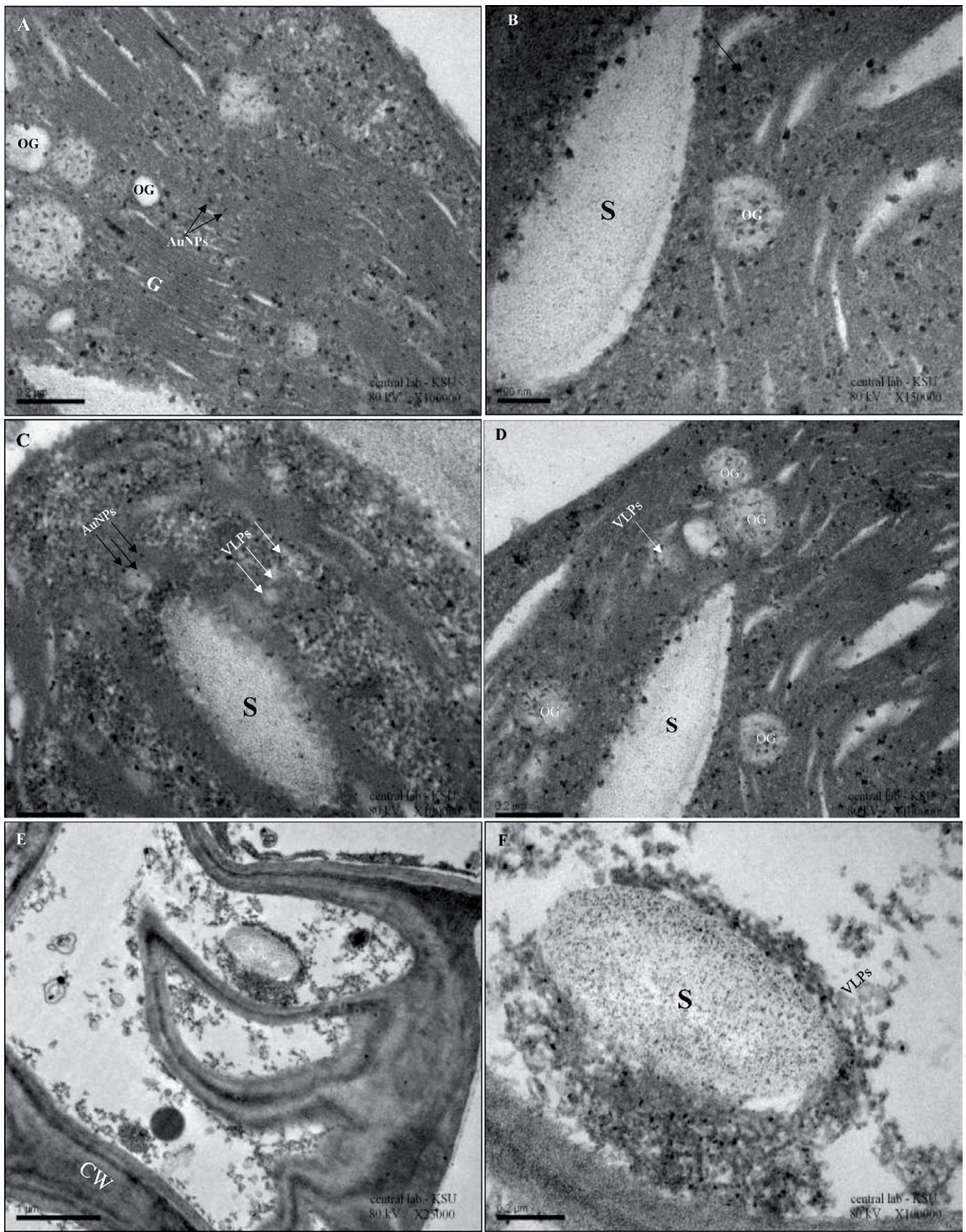

Figure 4.
Electron micrographs demonstrated many vesicles and starch body in the chloroplast. **(A)** *Noticed the grana was not striated and filled with light OG and having a lot of starch granules, Scale bar 0.2 μm.* **(B)** *Higher magnification from A, Scale bar 100 nm.* **(C)** *Starch granules surrounded by virus-like particles (VLPs) and gold nanoparticles (AuNPs) in the chloroplast in a highly magnified part of the grana, Scale bar 0.2 μm.* **(D)** *Micrograph of the grana decomposition in chloroplast showed the OG, which turned to hollow vesicles and filled with some cell material and VLPs from the virus-infected. (Outlined some aggregated VLPs), Scale bar 0.2 μm. Electron micrographs demonstrated the late stage of plasmolysis in the chloroplast.* **(E)** *Abnormal deformed invagination of the cell wall with remained starch body according to plasmolysis inside the cell. Scale bar 1 μm.* **(F)** *Plasmolysis of chloroplast with remained one starch granules surrounded by Nanoparticles associated with some VLPs., Scale bars 0.2 μm.*
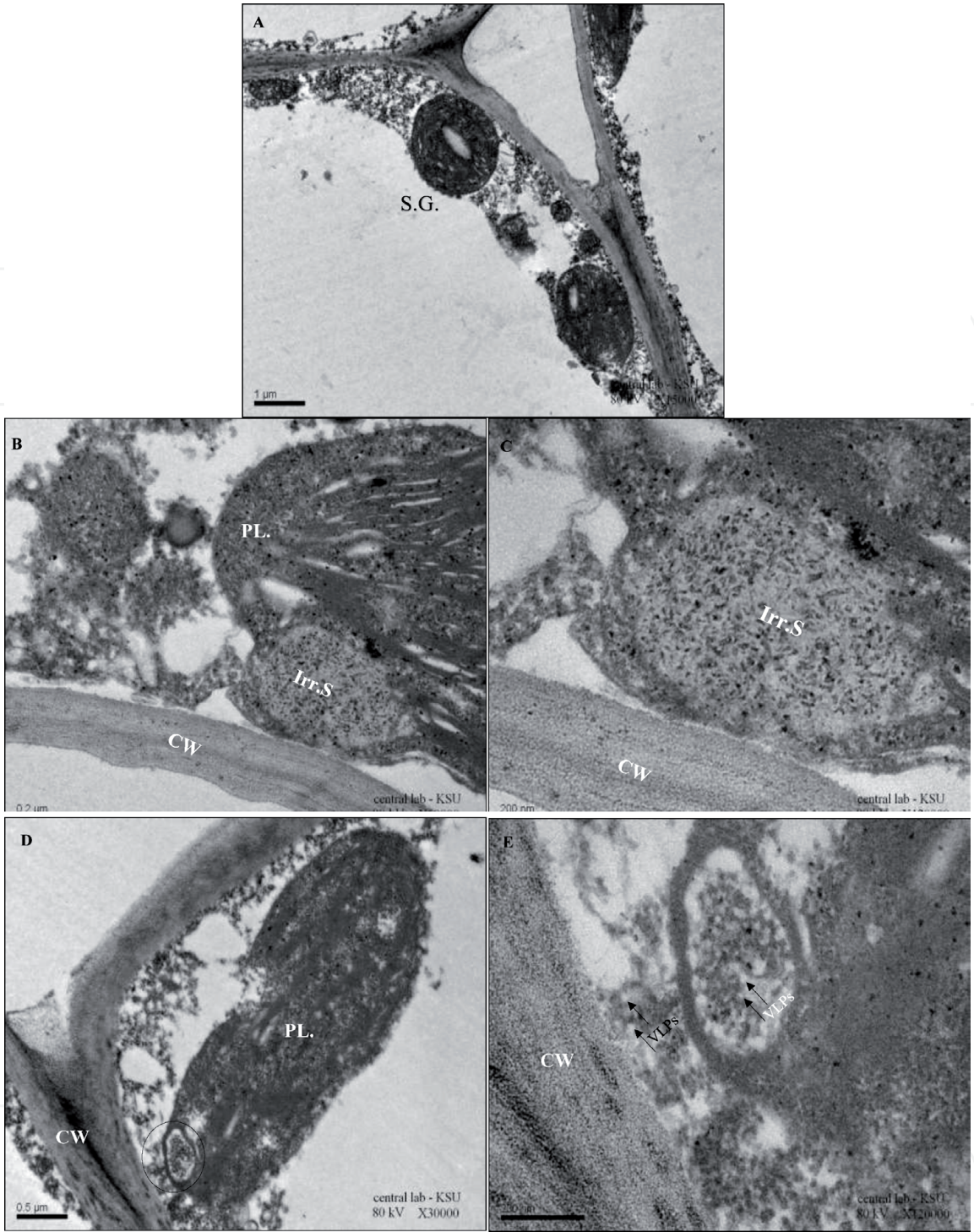
Figure 5.
Micrographs of different abnormalities in the plastid; rounded chloroplast. (A) Micrograph of abnormally rounded chloroplast with one starch granules. Scale bar 1 μm. Micrographs of different abnormalities in the plastid; irregular starch granules (B) The cell contains an abnormal amorphous material adjacent both plastid and cell wall, Scale bars 0.2 μm (C) higher magnification showed this material having portentous contents with different irregular starch granules with many AuNPs. Scale bar 200 nm. Micrographs of different abnormalities in the plastid; deformed and decomposed chloroplast. (D) Elongated and tiered in the chloroplast with (OG) and have some hollow (circle outlined) surrounded part near the border of the plastid, some VLPs were located beside these hollow, Scale bar 0.5 μm. (E) a higher magnification illustrated the content of vacuole having many VLPs inside, outside and near the cell wall (arrow) indicted VLPs, Scale bar 200 nm.

abscisic acid, jasmonic acid, methyl jasmonate, methyl salicylate (MS), and salicylic acid (SA) following BYDV infection. They followed the phytohormones over time and with different watering conditions than undamaged controls and seedlings infested with non-viruliferous aphids. Total hormone concentrations in BYDV-infected plants

were more significant than those in sham-treated and control plants. SA was higher in infected plants, but MS was low.

Turnip yellow mosaic virus (TYMV) replication machinery interacts with the outer membrane of infected cell chloroplasts [32], like in our study in **Figure 5(A, B, D,** and **E)**. In TYMV-infected cells, the chloroplasts adopt a cup-shaped form aggregate and swell. Two TYMV proteins are targeted to the chloroplast membrane and are involved in these processes, the 66 and 140 kDa proteins. The 140 kDa protein induces chloroplast aggregation and induces the invagination of the outer chloroplast membrane to form small peripheral vesicles, which are the sites of TYMV replication. Invaginations of endoplasmic and the plastid membrane were precise in our micrographs; **Figures 2(A)** and **(B)** and **4(A)**.
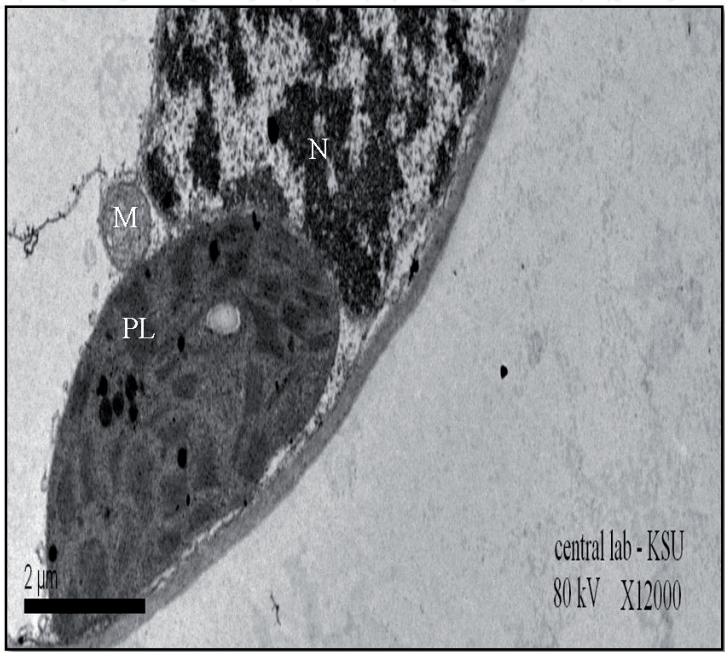

Figure 6.
The mitochondrion is a semi-autonomous double-membrane-bound organelle in this figure. Mitochondria are commonly measured between 0.75 and 3 μm² in the area but vary considerably in size and structure. The organelle is composed of compartments; these compartments include the outer membrane, the intermembrane space, the inner membrane, and the cristae and matrix. Scale bar 2 μm.
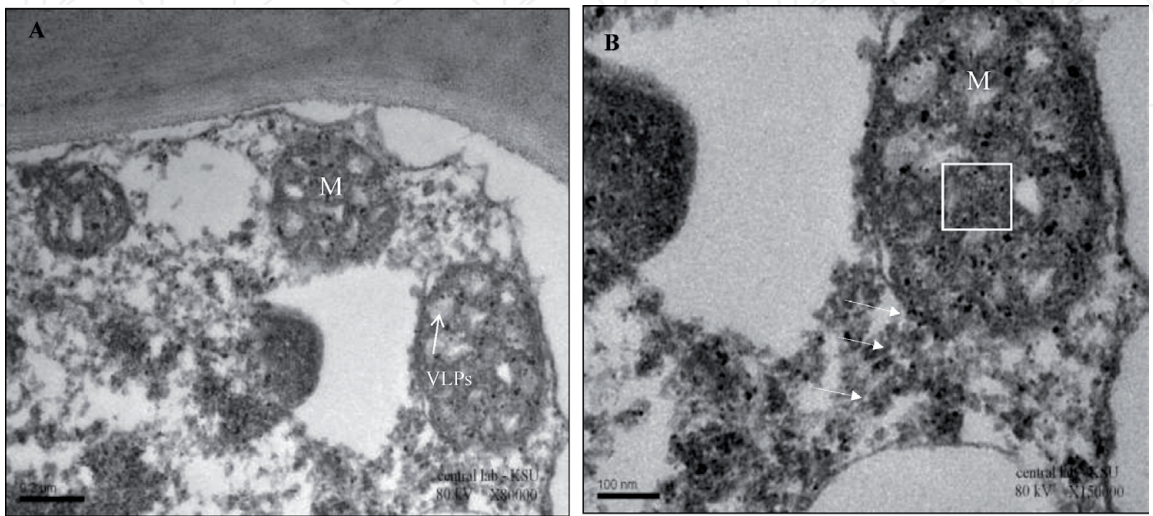

Figure 7.
*Micrographs of a distorted mitochondrion with internal membrane-bound areas containing amorphous inclusion bodies. (**A and B**) A lot of amorphous inclusion bodies (outlined) inside and outside the mitochondria with virus-like particles VLPs (arrows), Scale bars 0.2 μm, 100 nm.*
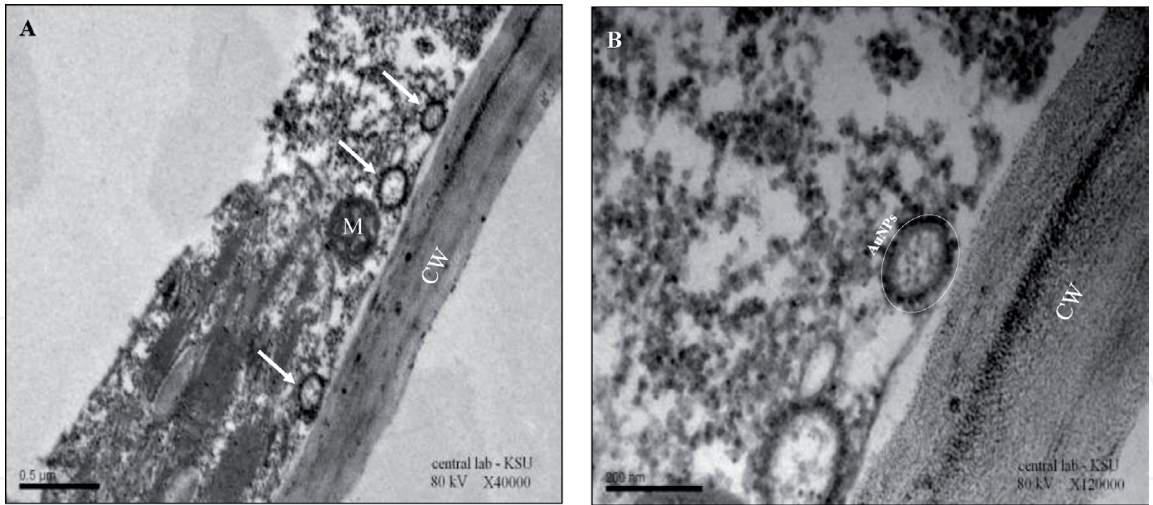
Figure 8.
*Micrographs of localized and precipitated AuNPs around the mitochondria as shown in figure (**A**) with fewer compartments than the health and higher magnification of the deformed mitochondrial organ and the AuNPs exist inside and along the cell wall as shown in figure (**B**). Scale bars 0.2 μm and 200 nm.*

Mitochondria and plastids in infected cells became degenerate in a way similar to those in uninfected maturing sieve elements. Negative staining preparation for Electron Microscopy is used for staining virus particles and the morphological and cytological side of healthy (**Figure 6**) and treated leaves [33]. Some alterations were detected in mitochondria of fully infected phloem cells, **Figure 7 (A)** and **(B)**. Furthermore, virus-specific vesicles with the limiting membrane were developed in the cytoplasm.

Deformed mitochondrial organ with fewer compartments than the healthy and the AuNPs exist inside and along the cell wall, **Figure 8(A)** and **(B)**.

Abbreviations

BYDV-PAV	Barley Yellow Dwarf Virus
BYDV-GAV	Barley Yellow Dwarf Virus
ROS	Reactive Oxygen Species
ABA	Abscisic acid
ET	Ethylene
TMV	Tobacco mosaic virus
CP	Coat protein
EM	Electron microscope
TEM	Transmission electron microscope
AuNPs	Gold nanoparticles
TIO_2	Titanium Oxide
RCA	Rubisco activase
mRNA	Messenger Ribonucleic Acid
TiO_2NPs	Nano-anatase particles
MS	Methyl salicylate
SA	Salicylic acid
TYMV	Turnip yellow mosaic virus
KDA	kilodalton
S	Starch
OG	Osmophilic globule
MLB	Myelin like bodies
G	Grana

VLPs	Virus-like particles
CW	Cell wall
SG	Starch granules
IRR.S	Irregular starch granules
N	Nucleus
M	Mitochondria
PL	Plastid

Author details

Noorah Abdulaziz Othman Alkubaisi[1*] and Nagwa Mohammed Amin Aref[2]

1 Department of Botany and Microbiology, College of Science, King Saud University, Riyadh, Kingdom of Saudi Arabia

2 Department of Microbiology, College of Agriculture, Ain Shams University, Cairo, Egypt

*Address all correspondence to: nalkubaisi@ksu.edu.sa

IntechOpen

References

[1] S. Choudhury, H. Hu, H. Meinke, S. Shabala, G. Westmore, P. Larkin, M. Zhou, Barley yellow dwarf viruses: infection mechanisms and breeding strategies, Euphytica 213(8) (2017) 168.

[2] C. Gill, J. Chong, Development of the infection in oat leaves inoculated with barley yellow dwarf virus, Virology 66(2) (1975) 440-453.

[3] T. Zhou, A.M. Murphy, M.G. Lewsey, J.H. Westwood, H.-M. Zhang, I. Gonzalez, T. Canto, J.P. Carr, Domains of the cucumber mosaic virus 2b silencing suppressor protein affecting inhibition of salicylic acid-induced resistance and priming of salicylic acid accumulation during infection, The Journal of general virology 95(Pt 6) (2014) 1408.

[4] C. D'Arcy, L. Domier, M. Mayo, Family luteoviridae, Virus Taxonomy: VIIIth Report of International Committee on Taxonomy of Viruses (2005).

[5] K.H. Orwin, M.U. Kirschbaum, M.G. St John, I.A. Dickie, Organic nutrient uptake by mycorrhizal fungi enhances ecosystem carbon storage: a model-based assessment, Ecology Letters 14(5) (2011) 493-502.

[6] Y. Wang, R. Chen, Y. Hao, H. Liu, S. Song, G. Sun, Transcriptome analysis reveals differentially expressed genes (DEGs) related to lettuce (Lactuca sativa) treated by TiO 2/ZnO nanoparticles, Plant Growth Regulation 83(1) (2017) 13-25.

[7] W. Yu, H. Xie, Y. Li, L. Chen, Experimental investigation on thermal conductivity and viscosity of aluminum nitride nanofluid, Particuology 9(2) (2011) 187-191.

[8] F. Gao, F. Hong, C. Liu, L. Zheng, M. Su, X. Wu, F. Yang, C. Wu, P. Yang, Mechanism of nano-anatase TiO 2 on promoting photosynthetic carbon reaction of spinach, Biological trace element research 111(1-3) (2006) 239-253.

[9] X. Ma, R. Jian, P.R. Chang, J. Yu, Fabrication and characterization of citric acid-modified starch nanoparticles/plasticized-starch composites, Biomacromolecules 9(11) (2008) 3314-3320.

[10] M. Qi, Y. Liu, T. Li, Nano-TiO 2 improve tomato leaves' photosynthesis under mild heat stress, Biological trace element research 156(1-3) (2013) 323-328.

[11] M. Nasrollahzadeh, M.S. Sajadi, M. Atarod, M. Sajjadi, Z. Isaabadi, An Introduction to Green Nanotechnology, Academic Press2019.

[12] A.O. Govorov, I. Carmeli, Hybrid structures composed of the photosynthetic system and metal nanoparticles: plasmon enhancement effect, Nano letters 7(3) (2007) 620-625.

[13] E. Cabiscol, J. Ros, Oxidative damage to proteins: structural modifications and consequences in cell function, Redox proteomics: from protein modification to cellular dysfunction and disease (2006) 399-471.

[14] V. Chinnusamy, J.-K. Zhu, Epigenetic regulation of stress responses in plants, Current opinion in plant biology 12(2) (2009) 133-139.

[15] S.T. Thul, B.K. Sarangi, Implications of nanotechnology on plant productivity and its rhizospheric environment, Nanotechnology and plant Sciences, Springer2015, pp. 37-53.

[16] M.H. Siddiqui, M.H. Al-Whaibi, M. Firoz, M.Y. Al-Khaishany, Role of nanoparticles in plants, Nanotechnology and Plant Sciences, Springer 2015, pp. 19-35.

[17] N. Verbruggen, C. Hermans, H. Schat, Molecular mechanisms of metal hyperaccumulation in plants, New phytologist 181(4) (2009) 759-776.

[18] J.A. Lemire, J.J. Harrison, R.J. Turner, Antimicrobial activity of metals: mechanisms, molecular targets, and applications, Nature Reviews Microbiology 11(6) (2013) 371-384.

[19] V. Kumar, P. Guleria, V. Kumar, S.K. Yadav, Gold nanoparticle exposure induces growth and yield enhancement in Arabidopsis thaliana, Science of the total environment 461 (2013) 462-468.

[20] S. Arora, P. Sharma, S. Kumar, R. Nayan, P. Khanna, M. Zaidi, Gold-nanoparticle induced enhancement in growth and seed yield of Brassica juncea, Plant Growth Regulation 66(3) (2012) 303-310.

[21] W. Rong, X. Wang, X. Wang, S. Massart, Z. Zhang, Molecular and ultrastructural mechanisms are underlying yellow dwarf symptom formation in wheat after infection of Barley Yellow Dwarf Virus, International Journal of molecular sciences 19(4) (2018) 1187.

[22] W.A. Miller, S. Dinesh-Kumar, C.P. Paul, Luteovirus gene expression, Critical Reviews in plant sciences 14(3) (1995) 179-211.

[23] S.G. Jensen, Metabolism and Carbohydrate Composition in Barley, Phytopathology 62 (1972) 587-592.

[24] W.E. Riedell, R.W. Kieckhefer, M.A. Langham, L.S. Hesler, Root and shoot responses to bird cherry-oat aphids and barley yellow dwarf virus in spring wheat, Crop Science 43(4) (2003) 1380-1386.

[25] S.G. Jensen, J.W. Van Sambeek, Differential effects of barley yellow dwarf virus on the physiology of tissues of hard red spring wheat, Phytopathology 62 (1972) 290-293.

[26] S. Jensen, P. Fitzgerald, J. Thysell, Physiology and Field Performance of Wheat Infected with Barley Yellow Dwarf Virus 1, Crop Science 11(6) (1971) 775-780.

[27] A. Marquardt, G. Scalia, P. Joyce, J. Basnayake, F.C. Botha, Changes in photosynthesis and carbohydrate metabolism in sugarcane during the development of Yellow Canopy Syndrome, Functional plant biology 43(6) (2016) 523-533.

[28] P. Klein, C.M. Smith, Host plant selection and virus transmission by Rhopalosiphum maidis are conditioned by potyvirus infection in Sorghum bicolor, Arthropod-Plant Interactions (2020) 1-13.

[29] I. Łukasik, A. Wołoch, H. Sytykiewicz, I. Sprawka, S. Goławska, Changes in the content of thiol compounds and the activity of glutathione s-transferase in maize seedlings in response to a rose-grass aphid infestation, PloS one 14(8) (2019) e0221160.

[30] H. Sytykiewicz, P. Czerniewicz, I. Sprawka, R. Krzyzanowski, Chlorophyll content of aphid-infested seedling leaves of fifteen maize genotypes, Acta Biologica Cracoviensia. Series Botanica 55(2) (2013).

[31] D.W. Mornhinweg, S. Ullrich, Biotic stress in barley: Insect problems and solutions, Barley: Production, improvement, and uses (2011) 355-390.

[32] D. Prod'homme, A. Jakubiec, V. Tournier, G. Drugeon, I. Jupin, Targeting the turnip yellow mosaic virus 66K replication protein to the chloroplast envelope is mediated by the 140K protein, Journal of virology 77(17) (2003) 9124-9135.

[33] J. Kuo, Electron microscopy: methods and protocols, Springer Science & Business Media 2007.